

Effect of MgO, Y₂O₃, and Fe₂O₃ on silicothermal synthesis and sintering of X-sialon. An XRD, multinuclear MAS NMR and ⁵⁷Fe Mössbauer study

K.J.D. MacKenzie^{a,*}, C.M. Sheppard^a, C. McCammon^b

^aNew Zealand Institute for Industrial Research and Development, PO Box 31-310 Lower Hutt, New Zealand

^bBayerisches Geoinstitut, Universität Bayreuth, D-95440 Bayreuth, Germany

Received 25 October 1999; received in revised form 3 April 2000; accepted 8 April 2000

Abstract

The separate effects of 10 wt.% MgO, Y₂O₃ and Fe₂O₃ on the silicothermal formation and sintering of X-sialon were investigated by XRD, multinuclear MAS NMR and Mössbauer spectroscopy. The effects of the three oxides on densification follow a similar trend to samples containing 1 wt.% oxide (Y > Mg > Fe), but at the higher additive concentration, the maximum densities are higher and are achieved at lower temperature (1400°C). 10 wt.% MgO and Y₂O₃ facilitate low-temperature mullite formation and its conversion to X-sialon by forming increased amounts of liquid phases. The ²⁵Mg NMR spectra of the MgO-containing samples suggest that their liquid phase is a N-containing Mg silicate glass. These samples also form MgAl₂O₄, depleting the amount of Al available to form X-sialon. The Y₂O₃-containing samples form liquid of a similar composition to N-melilite, depleting the available Si, with the excess alumina appearing as corundum. Under silicothermal conditions, Fe₂O₃ reacts with the Si to form a mixture of magnetic silicide and aluminide, suppressing X-sialon formation by depleting the Si but enhancing the formation and stability of mullite by Fe-for Al substitution in the mullite lattice. Some of the magnetic phases may occur as very fine superparamagnetic particles possibly located in an X-sialon matrix. © 2000 Elsevier Science Ltd. All rights reserved.

Keywords: Additives; NMR; Phase development; Sialon; Sintering; X-ray methods

1. Introduction

X-sialon, Si₁₂Al₁₈O₃₉N₈, is a silicon aluminium oxynitride phase with a structure similar to that of mullite (Al₆Si₂O₁₃). Sintered X-phase bodies have been found¹ to have mechanical properties comparable with those of other sialons, silicon nitrides and mullite, and good chemical stability to ferrous alloys at 1200°C.² We have previously reported a silicothermal synthesis method for X-sialon³ using pure kaolinite or halloysite, elemental silicon powder and γ-alumina to adjust the composition of the mixture. The silicothermal reaction sequence involves several parallel steps (nitridation of the Si to Si₃N₄, decomposition of the kaolinite to mullite and amorphous silica, reaction between the γ-alumina and the amorphous silica to form more mullite, and reaction

between the mullite and Si₃N₄ to form sialon).³ We have also reported⁴ the effect on the synthesis and densification of a number of metal oxides added at low concentration (1 wt.%) in which we found that Y₂O₃ and MgO were beneficial to both the formation of crystalline X-sialon and to its subsequent densification. The effect of these two oxides on the formation of X-sialon is related to their effect on the conversion of the initially-formed SiN₄ units to SiO₂N₂ and SiO₃N units,⁴ which is especially facilitated by Y₂O₃. The sintering of X-sialon, which is particularly influenced by MgO at lower temperatures, appears to be related to the formation of liquid phases.⁴ The effect of Fe₂O₃ on the silicothermal reaction was interesting; although it assists the initial stage of the reaction (nitridation of the silicon), it suppresses subsequent X-sialon formation by stabilising the preceding mullite phase.

At additive concentrations of 1 wt.%, the amounts of glass and minor phases formed are very small, making them difficult to study by XRD and MAS NMR. It was, therefore, decided to investigate further the effects on the reaction sequence of the three more interesting oxides

* Corresponding author at present address: Department of Materials, University of Oxford, Parks Road, Oxford OX1 3PH, UK. Tel.: +44-1865-273700; fax: +44-1865-273789.

E-mail address: kenneth.mackenzie@materials.ox.ac.uk (K.J.D. MacKenzie).

by increasing their concentration to 10 wt.%. The advantage of this high additive concentration is that it opens up the possibility of direct observation of the changes in the environment of the doping cations by spectroscopic techniques specific to the cation (^{25}Mg and ^{89}Y MAS NMR and ^{57}Fe Mössbauer spectroscopy). Since the use of an additive content which is higher than might be contemplated in a manufacturing situation could lead to changes in the minor phases formed, this possibility was examined by a qualitative comparison of the present results with those obtained previously using 1 wt.% oxide additions.

The technique of solid state nuclear magnetic resonance spectroscopy with magic angle spinning (MAS NMR) has provided useful information on the behaviour of nuclides such as ^{27}Al and ^{29}Si during the processing of a number of ceramic materials including sialons.⁵ By contrast with X-ray diffraction, which depends on the presence of long-range order in the crystal structure, MAS NMR detects the immediate bonding of the various atoms, thereby providing complementary information on the composition of the structural units present irrespective of the crystallinity of the phases in which they occur. MAS NMR of ^{25}Mg and ^{89}Y is more difficult than ^{27}Al and ^{29}Si , but has been successfully used to provide information about the effect of these oxide additives on the sintering of silicon nitride⁶ and β -sialon.⁷ The presence of more than about 5% Fe in a sample generally gives rise to large spinning side bands, militating against MAS NMR studies; Mössbauer (γ -ray) spectroscopy is the preferred technique for investigating such materials, and was used to study the present iron-containing samples.

2. Experimental

The starting materials were as used in the previous study⁴ (halloysite clay supplied by NZ China Clays Ltd, elemental silicon powder (Permascand 4D) and γ -alumina prepared by dehydroxylating a British Drug Houses reagent grade $\text{Al}(\text{OH})_3$ at 800°C for 3.5 h.). These constituents were mixed in proportions to give the X-phase composition $\text{Si}_{12}\text{Al}_{18}\text{O}_{39}\text{N}_8$ and ball-milled for 20 h in hexane as previously described.⁴ The oxides MgO , Y_2O_3 and Fe_2O_3 were added to the milled feedstock at a concentration of 10 wt.% of the final sialon yield, assuming complete formation of X-sialon. The mixtures were homogenised by hand grinding under ethanol and uniaxially pressed at 140 MPa into 10 mm dia. pellets. Firings were carried out in purified flowing nitrogen (100 ml min^{-1}) at a heating rate of 5°C min^{-1} to 1100°C , then 2°C min^{-1} to the maximum temperature as detailed elsewhere.⁴ On reaching the maximum firing temperature, the furnace was cooled immediately, with no holding period at temperature. This was intended to provide a “snapshot” of the progress of the reaction at each

temperature rather than to attempt to approach equilibrium conditions at each temperature. This procedure also allowed a direct comparison to be made with previously reported results⁴ for mixtures containing 1 wt.% of these additives. The pellet faces were lapped on a diamond wheel and examined by XRD (Philips PW 1700 computer-controlled diffractometer with CoK_α radiation and a graphite monochromator). After measurement of bulk densities and open porosity by water absorption, the pellets were ground and examined as appropriate by solid state ^{29}Si , ^{27}Al , ^{25}Mg and ^{89}Y MAS NMR at 11.7T using a Varian Unity 500 spectrometer with a 5 mm Doty MAS probe spun at 10–12 kHz. The spectra were acquired under the following conditions: ^{29}Si : $6\text{ }\mu\text{s}$ $\pi/2$ pulse with a recycle delay of 100 s, spectra referenced to tetramethylsilane (TMS); ^{27}Al : $1\text{ }\mu\text{s}$ $\pi/10$ pulse for solution with a recycle delay of 5 s, spectra referenced to 1 M aqueous $\text{Al}(\text{NO}_3)_3$ solution; ^{25}Mg : $3\text{ }\mu\text{s}$ $\pi/10$ pulse for solution with a recycle delay of 0.1 s, $90\text{ }\mu\text{s}$ ringdown delay prior to acquisition as discussed elsewhere,⁸ spectra referenced to 1 M aqueous MgSO_4 solution; ^{89}Y : $20\text{ }\mu\text{s}$ $\pi/2$ pulse, recycle delay of 3 s, $170\text{ }\mu\text{s}$ ringdown delay between excitation and sampling, spectra referenced to aqueous YCl_3 solution. Although the addition of a small amount of paramagnetic species such as lanthanide ions is usually advisable to facilitate the detection of ^{89}Y by increasing its relaxation rate,⁹ this procedure was not found to be necessary with the present samples, probably due to the presence of naturally occurring paramagnetic species in the reactants.

Mössbauer spectroscopy was carried out on the iron-containing samples by mounting the powders in Plexiglass sample holders such that 5 mg Fe cm^{-2} was presented to the γ -ray beam. The spectra were recorded at room temperature (293 K) in transmission mode on a constant acceleration Mössbauer spectrometer with a nominal 50 mCi ^{57}Co source in a $6\text{ }\mu\text{m}$ Rh matrix. The velocity scale was calibrated relative to 25-micron α -Fe foil using the positions certified for the NBS standard reference material no. 1541. Line widths of 0.28 mm s^{-1} were obtained at room temperature for the outer lines of α -Fe. The spectra were fitted to Lorentzian lineshapes using the commercially available fitting program NORMOS written by R. A. Brand (distributed by Wissenschaftliche Elektronik GmbH, Germany).

3. Results and discussion

3.1. Effect of additives on sintering behaviour

The bulk densities of the fired pellets as a function of temperature are shown in Fig. 1.

The beneficial effects of Y_2O_3 and MgO (Fig. 1A) follow the same trends as previously found with 1 wt.% additive concentration (Fig. 1B), but with overall higher

densities recorded at 1500°C, especially with Y_2O_3 , for which the 1500°C densities at 1 and 10 wt.% are 2.7 and 3.2 g cc⁻¹ respectively. The tailing-off of the density curves for samples containing 10 wt.% Y_2O_3 and MgO above 1400°C indicates the temperature at which they approach theoretical density at this additive concentration. The slight retardation of sintering found below 1400°C with the present concentration of Fe_2O_3 by comparison with the control sample (Fig. 1A) is consistent with the result previously found with 1 wt.% of this additive over the whole temperature range.⁴ As found with the lower additive concentration, the shrinkage curves mirror the density curves, and all the plots of apparent porosity show inverse behaviour; the porosity of the Y_2O_3 -containing samples decreases rapidly between 1300 and 1400°C and approaches zero at 1400°C, with a similar decrease to approximately zero porosity occurring at 1500°C in the MgO-containing samples. By contrast, the porosities of the control and Fe_2O_3 -containing samples remain high even at 1500°C (33.5 and 37% respectively). Thus, the trends in the sintering behaviour are independent of additive concentration, but the final densities are greater with 10 wt.% additive, especially for the high molecular weight Y_2O_3 , as would be expected.

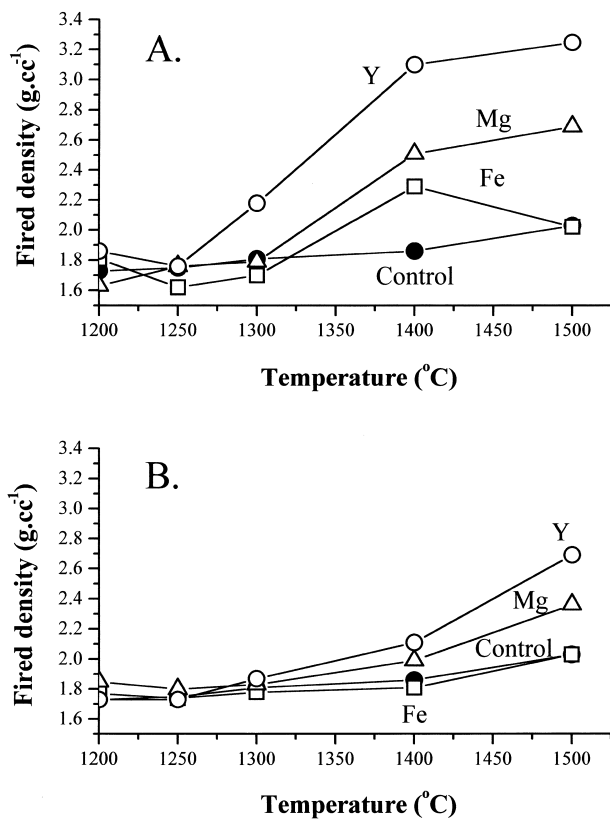


Fig. 1. Fired densities of sintered silicothermal X-sialon pellets with and without oxide additives. A. 10 wt.% additive. B. 1 wt.% additive (data from Ref. 4).

3.2. X-ray diffraction of the crystalline phases

The effects of the oxide additives on the formation of X-sialon and its major precursor phase mullite are shown in Fig. 2, in which a semi-quantitative estimate of phase development is taken as the relative intensity of its most significant unobstructed diffraction peak (the 100 X-sialon reflection at $d=3.62$ Å and the 110 mullite reflection at $d=5.39$ Å).

The trends shown in Fig. 2 are generally similar to those previously found with lower additive concentrations. Low-temperature formation of mullite and its subsequent conversion to X-sialon is facilitated by both Y and Mg (Fig. 2A) but the relative amount of mullite formed and the temperature at which it begins to decrease are both lowered by the increased content of these two additives. By contrast, the presence of a high Fe content produces a continuous increase in mullite formation with temperature, with no sign of the decrease due to X-sialon formation even at 1500°C (Fig. 2A). This result, which is consistent with the previous findings at lower additive concentration, has been interpreted⁴ in terms of the stabilisation of the mullite structure by Fe. These conclusions are consistent with the formation behaviour of X-sialon (Fig. 2B), which is

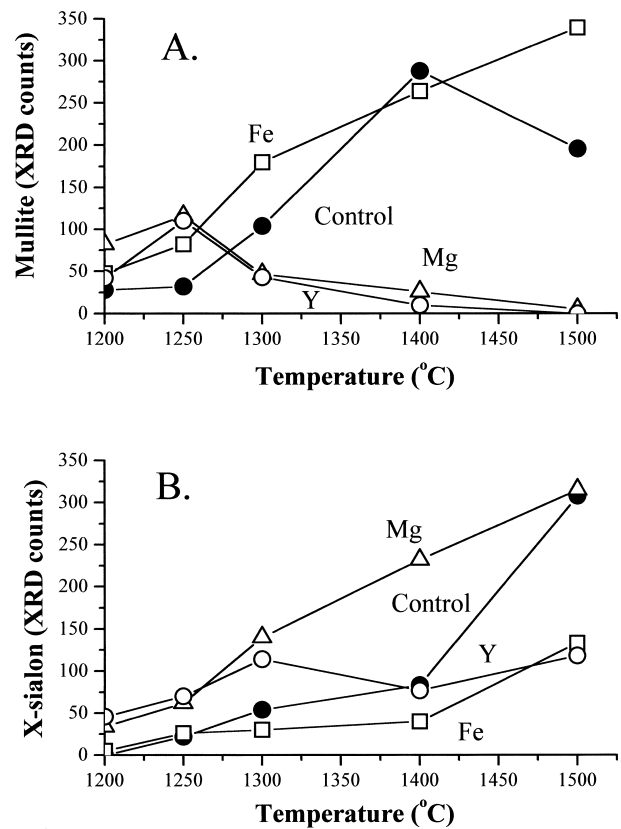


Fig. 2. Temperature dependence of phase formation in silicothermal X-sialon pellets containing 10 wt.% oxide additives by semi-quantitative XRD. A. Mullite; B. X-sialon.

facilitated by Mg and retarded by Fe. The behaviour of the Y-containing material is, however, anomalous; the amount of X-sialon formed relative to the control sample is lower than with 1 wt.% additive, and the early removal of mullite is not accompanied by a corresponding increase in X-sialon content (Fig. 2), suggesting the preferential formation of some other yttrium-containing phase.

Fig. 3 shows the XRD traces for the additive-containing samples and the control sample without additives, fired at 1500°C.

The major phase in the control sample (Fig. 3A) is X-sialon (PDF no.36-832), with a significant amount of

unreacted mullite (PDF no.15-776) and a small amount of O'-sialon (PDF no. 42-1492).

The crystalline phases formed at 1500°C in samples containing 10 wt.% MgO (Fig. 3B) are X-sialon and a significant quantity of spinel, $MgAl_2O_4$ (PDF no. 21-1152) which replaces the mullite found in the control sample. A small trace of enstatite, $MgSiO_3$ (PDF no. 34-1216) may also be present.

Samples containing 10 wt.% Y_2O_3 (Fig. 3C) form crystalline X-sialon at 1500°C, together with a considerable amount of α -alumina (PDF no. 10-173) and O'-sialon. There is no indication of any crystalline Y-containing phases such as yttrium aluminium garnet (YAG) or yttrium silicates, but the noisy XRD baseline may conceal the presence of a glassy phase containing the yttrium and some of the silica. The removal of the latter from the mullite and sialon by glass formation would explain the high concentration of α -alumina observed in this sample.

The sample containing 10 wt.% Fe_2O_3 shows only a small amount of X-sialon formation at 1500°C (Fig. 3D), the major crystalline phases being mullite and iron silicides; although the composition of the latter is difficult to identify by XRD, it could correspond to Fe_3Si (PDF no. 45-1207) or $FeSi$ (PDF no. 38-1397) or a mixture of silicides.

The development of these phases as a function of firing temperature is shown semi-quantitatively in Fig. 4.

The additive-free control samples (Fig. 4A) show a rapid removal of silicon at 1250–1300°C by nitridation and sialon formation. X-sialon develops slowly up to 1400°C by reaction between the γ -alumina and silicon nitride. Above 1400°C the steeply increasing growth of X-sialon begins to consume some of the mullite which up to that temperature has been increasing continuously, initially as a result of thermal decomposition of the clay, but at higher temperatures, by reaction of the γ -alumina with the amorphous silica from the clay. The small amount of α -alumina (corundum) which appears briefly at 1400°C arises from the unconsumed γ -alumina present at that temperature. The continuous presence of a small amount of O-sialon over the whole temperature range suggests that this is a secondary product rather than an intermediate.

The effect of adding 10 wt.% MgO (Fig. 4B) is to lower the onset temperature of significant X-sialon, probably by the formation of a low-melting liquid which facilitates transport of the reactants. Mullite formation is also restricted to that resulting from the primary decomposition of the clay since the formation of magnesium aluminate spinel consumes the additional alumina, suppressing the further formation of mullite by reaction between the amorphous silica and available alumina. Thus, the reaction sequence in the presence of a high concentration of MgO is dominated at higher temperatures by the preferential formation of spinel which

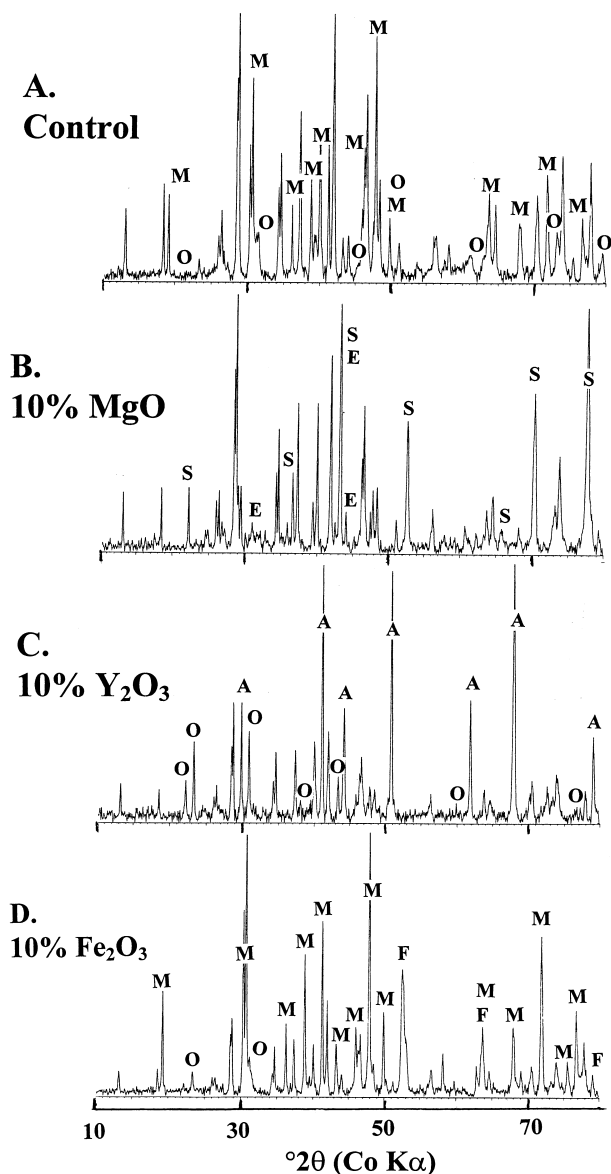


Fig. 3. XRD traces of silicothermal X-sialon pellets fired at 1500°C with and without 10 wt.% oxide additives. Key: M = mullite (PDF no. 15-776), O = O'-sialon (PDF no. 42-1492), S = $MgAl_2O_4$ spinel (PDF no. 21-1152), E = enstatite, $MgSiO_3$ (PDF no. 34-1216), A = α -alumina (PDF no. 10-173), F = Fe_3Si (PDF no. 45-1207). The unlabelled peaks correspond to X-sialon (PDF no. 36-832).

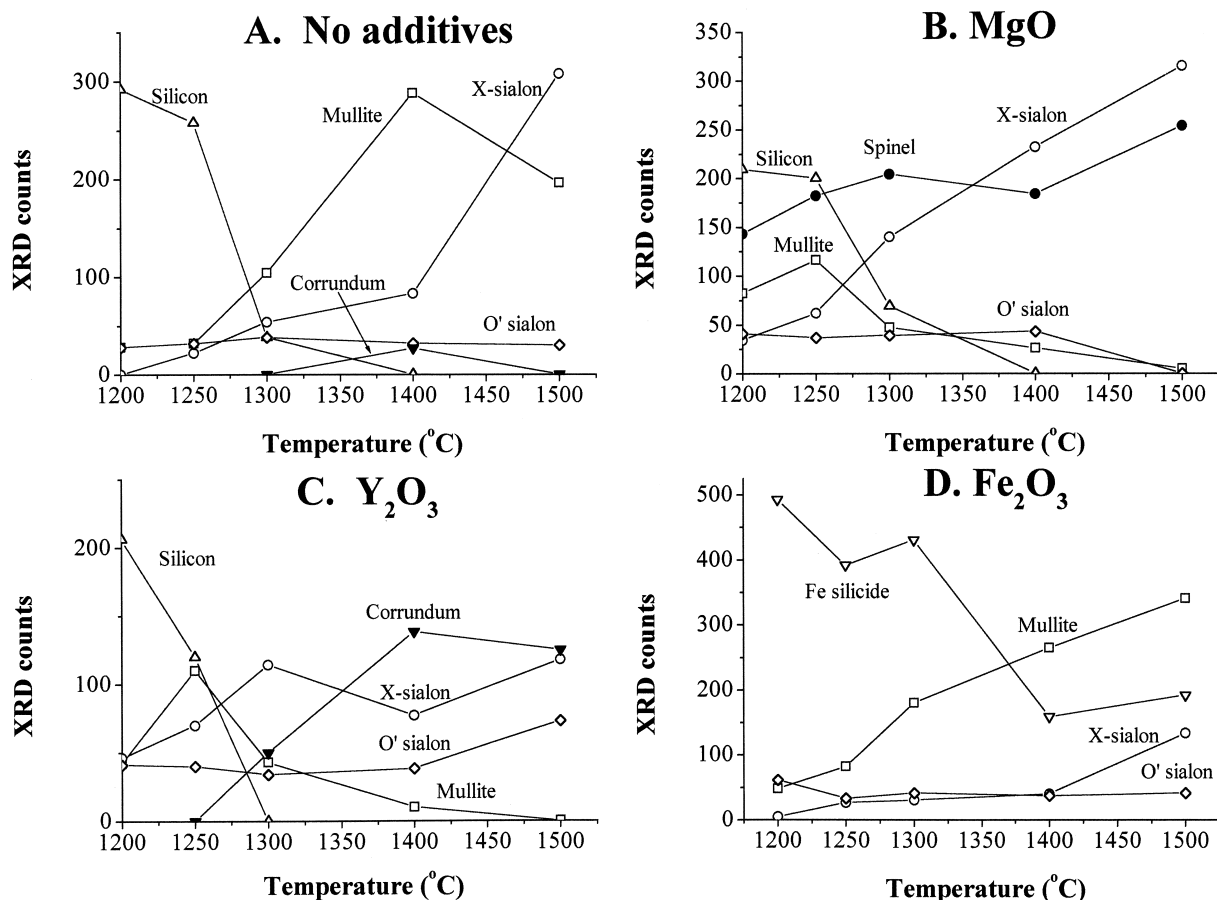


Fig. 4. Temperature dependence of phase formation in silicothermal X-sialon pellets with and without 10 wt.% oxide additives. A. Control, B. MgO, C. Y_2O_3 , D. Fe_2O_3 .

removes from the system the alumina necessary to sustain sialon formation.

By contrast, the action of 10 wt.% Y_2O_3 may be explained in terms of its removal of silica from the system by forming an yttrium-rich silicate liquid. This liquid facilitates the lower-temperature formation of X-sialon (Fig. 4C), which cannot however be maintained due to the depletion of the necessary silicon component. The resulting excess alumina appears as corundum (Fig. 4C).

The action of 10 wt.% Fe_2O_3 is characterised by the low-temperature reaction of the silicon starting material to form iron silicides, suppressing sialon formation by removing the necessary Si (Fig. 4D). Mullite formation and stability is also promoted by the entry of the iron into the mullite structure,¹⁰ further militating against sialon formation.

3.3. MAS NMR of the oxide-containing samples

3.3.1. 10 wt.% MgO

A series of typical ^{29}Si MAS NMR spectra are shown in Fig. 5A–E.

The sample fired at 1200°C contains three major resonances (Fig. 5A) corresponding to silicon oxynitride

units (−61 ppm), mullite-type Si–O–Al units (−87 ppm) and uncombined SiO_2 (−111 ppm). Firing at 1300°C reduces the intensity of the silica and mullite-type resonances as expected, and increases the intensity and resolution of a resonance at −55 ppm (Fig. 5C) corresponding to an increase in the number of SiO_2N_2 units.³ In the heating interval 1300–1400°C the ^{29}Si spectrum abruptly broadens and assumes the appearance of an X-sialon spectrum,³ with the development of a continuum of resonances centred on the SiO_3N resonance at −66 ppm. The spectrum of the sample heated at 1500°C (Fig. 5E) is typical of well-developed X-sialon, but with a greater prominence of the SiO_2N_2 resonance which appears to be favoured by higher MgO contents.

A typical ^{27}Al MAS NMR spectrum is shown in Fig. 5K. Its general features are unchanged over the present temperature range, with the octahedral resonance position remaining constant at 6.3 ppm, but a small progressive change in the position of the larger of the two overlapping tetrahedral resonances from about 62 ppm at 1200°C to 68 ppm at 1500°C. The tetrahedral:octahedral ratio and peak positions of these spectra are more typical of $MgAl_2O_4$ than of X-sialon, which contains a greater number of tetrahedral sites, and octahedral and tetrahedral

peak positions of about 0 and 62 ppm respectively.³ The Al spectra, therefore, remain predominately spinel type throughout the reaction, reflecting the easy transformation of the initial γ -alumina to MgAl_2O_4 by diffusion of Mg into the existing cubic oxygen lattice.

The corresponding ^{25}Mg spectra are shown in Fig. 5F–J. Their general features, which remain unchanged throughout the reaction, consist of two resonances, one at about 30–49 ppm corresponding to Mg in tetrahedral sites, the other, at –37 to –56 ppm, corresponding to octahedral sites.^{6,7} These spectra are very similar to those reported in Si_3N_4 and β '-sialon sintered in the presence of MgO, in which they were identified with a glassy phase formed by direct reaction of Si_3N_4 with MgO.⁶ The similarity of these spectra to those of MgSiN_2 and MgAlSiN_3 was taken as an indication that this amorphous phase may be stabilised by nitrogen.⁶ Although unreacted MgO would appear as a sharp peak at 25–30 ppm,⁸ within the range of some of these spectra, it is not observed by XRD in any of the samples. However, XRD of the present samples indicates the presence of significant quantities of MgAl_2O_4 , which is reported¹¹

to show a tetrahedral ^{25}Mg resonance at 52 ppm. We have not previously been able to reproduce this result for MgAl_2O_4 , but such a resonance could be present in these spectra, in which it would contribute to the observed tetrahedral envelope.

To summarise, the MAS NMR spectra of the Mg-containing samples indicate the establishment at 1300–1400°C of a typical X-sialon Si–O–N environment in which however the SiO_2N_2 units are over-represented by comparison with normal X-sialon. Throughout the reaction the Al remains in the tetrahedral/octahedral environment typical of a spinel. In addition to taking part in spinel formation, at least some of the Mg remains throughout the reaction in a nitrogen-containing glassy phase.

3.3.2. 10 wt.% Y_2O_3

Typical spectra of these samples are shown in Fig. 6.

The ^{29}Si spectra (Fig. 6A–C) show the early development of silicon oxynitride units (–61 to –62 ppm) and mullite-type Al–O–Si (–87 ppm) but less uncombined SiO_2 (–108 ppm) than in samples with MgO. The shoulder at –48 ppm in samples heated < 1400°C (Fig.

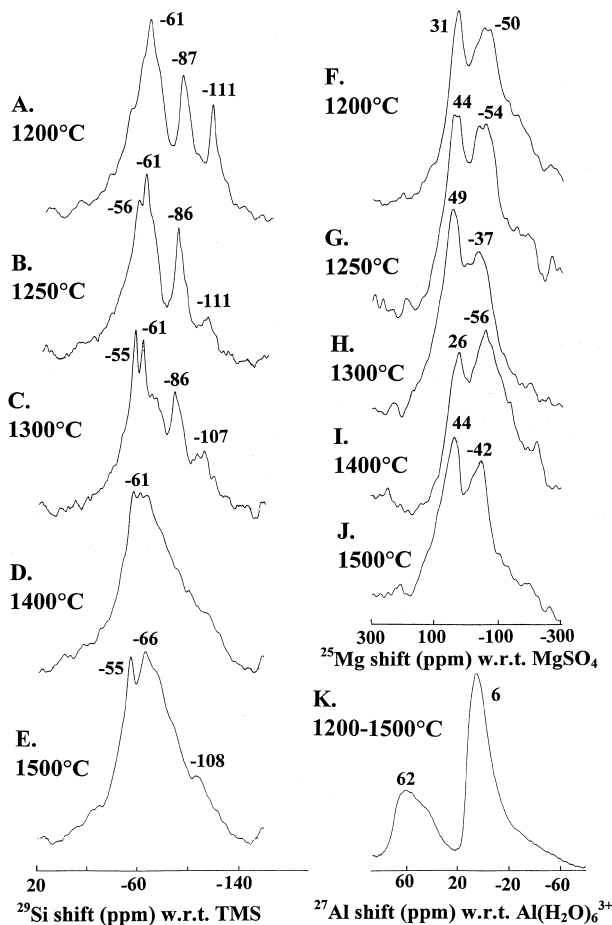


Fig. 5. Typical 11.7T MAS NMR spectra of silicothermal sialon reaction mixture containing 10 wt.% MgO. A–E. ^{29}Si spectra, F–J. ^{25}Mg spectra, K. ^{27}Al spectrum.

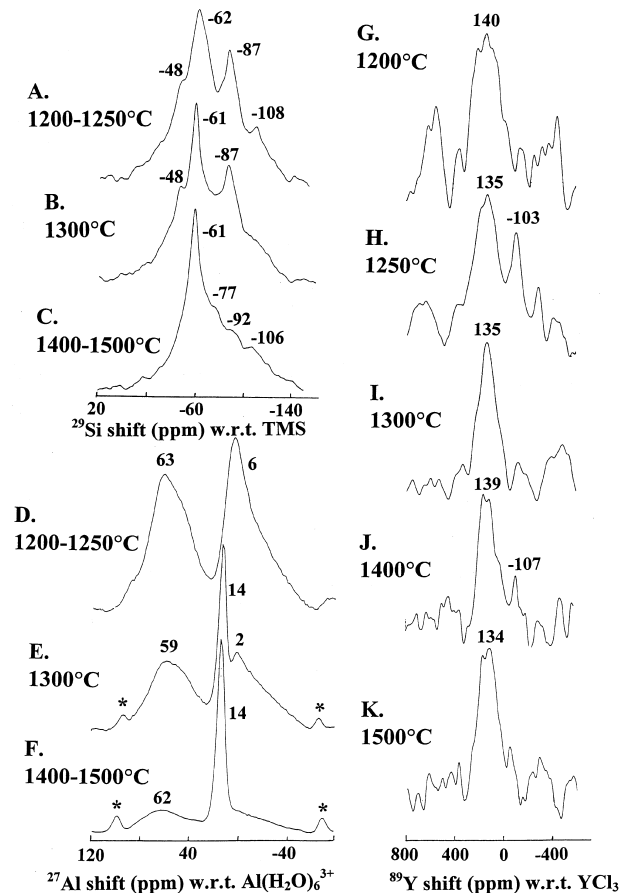


Fig. 6. Typical 11.7T MAS NMR spectra of silicothermal X-sialon reaction mixture containing 10 wt.% Y_2O_3 . A–C. ^{29}Si spectra, D–F. ^{27}Al spectra, G–K. ^{89}Y spectra. Asterisks denote spinning side bands.

6A and B) arises from unreacted Si_3N_4 . The spectra suggest that the high-temperature samples (Fig. 6C) contain a greater proportion of SiO_2N_2 units than in normal X-sialon, which shifts the position of the envelope maximum from about -67 ppm to -61 ppm. The predominance of SiO_2N_2 units may be explained by the presence of an amorphous phase with a composition similar to that of *N*-melilite ($\text{Y}_2\text{Si}_3\text{O}_3\text{N}_4$) which has a reported chemical shift of -56.7 ppm.¹² The formation of a yttrium-containing glass of this composition is also consistent with the ^{89}Y spectra (see below).

The ^{27}Al spectra (Fig. 6D–F) show at low temperatures the octahedral and tetrahedral resonances which occur both in mullite and γ -alumina spinel, but the peak positions are more like those of γ -alumina (66 and 7.6 ppm) than mullite (59 and 0.3 ppm), both measured under the same conditions.⁴ By 1300°C (Fig. 6E), the octahedral and tetrahedral peak positions have moved closer to the values for mullite, but the spectrum is changed by the abrupt appearance of the sharp octahedral resonance at 14 ppm arising from corundum (α -alumina) formed by thermal transformation of the unreacted γ -alumina. By 1400–1500°C (Fig. 6F) the spectrum is dominated by this resonance.

The corresponding ^{89}Y spectra (Fig. 6G–K) are broad and noisy, but show at lower temperatures a central peak at about 135–140 ppm. At 1400–1500°C (Fig. 6J and K), the central peak may show some evidence of multiple sites, but the centre-of-gravity remains at 134–139 ppm. This is in the general spectral region characteristic of *N*-melilite, $\text{Y}_2\text{Si}_3\text{N}_4\text{O}_3$ (160 ppm);⁹ it does not correspond to the resonances of yttrium aluminates (214–222 ppm),¹³ Y_2O_3 (272 and 314 ppm),¹³ or the yttrium silicates (198–237 ppm and 114–122 ppm).¹³ The absence of crystalline *N*-melilite from the XRD traces of these samples and the broadness of the NMR peaks suggests that throughout the reaction the yttrium remains in an amorphous oxynitride phase with a composition approaching $\text{Y}_2\text{Si}_3\text{N}_4\text{O}_3$, since the configuration of the atoms surrounding the Y (and hence the ^{89}Y chemical shift) is similar in both the crystalline and glassy phases of the same compound. The broadening in the glassy phase arises from the range of slightly different atomic environments present. These conclusions are also consistent with the ^{29}Si spectra.

To summarise, the MAS NMR spectra of the Y-containing samples show the early development of an amorphous yttrium silicon oxynitride phase containing predominately SiO_2N_2 units which persist to the highest temperature. The early appearance of this glassy phase, which is also confirmed by the ^{89}Y spectra, depletes the Si available for sialon formation and leads to the transformation of unreacted γ -alumina to corundum, evidenced by its characteristic ^{27}Al resonance. The formation of X-sialon at 1300–1400°C is indicated by the disappearance of the aluminosilicate resonance at -87 ppm.

3.3.3. 10 wt.% Fe_2O_3

Although the presence of such a high iron content makes NMR spectroscopy difficult by introducing major overlapping spinning side bands and the presence of magnetic components hinders the spinning of the samples in the magnetic field, an attempt was made to obtain ^{29}Si and ^{27}Al spectra from these samples. The resulting spectra were, however, too broad and noisy to provide much information about these samples. Valuable information specific to the iron present in the samples was, however, provided by Mössbauer spectroscopy.

3.4. ^{57}Fe Mössbauer spectroscopy of the 10 wt.% Fe_2O_3 samples

The Mössbauer spectra from four of the samples are shown in Fig. 7. All the spectra are very complex, consisting of several overlapping magnetic six-line features, with additional non-magnetic components contributing to the intensity of the inner parts of the spectra (at velocities between ca. -2 and $+2$ mm s⁻¹).

The approach to fitting these spectra was to find an adequate model with the least number of components. Attention was focused mainly on the prominent and best resolved peaks in the spectrum, and weaker features such as broad shoulders on peaks were not considered. The simplest model which fits all the prominent features consists of three magnetic sextets plus two quadrupole doublets. In addition, a 6-line magnetic spectrum corresponding to Fe_2O_3 was fitted to the spectrum of the sample fired at 1500°C (Fig. 7D) to take account of the weak features at about -8 and $+8$ mm s⁻¹ which correspond to the outer peaks of this phase.

The results of this fitting procedure are shown in Fig. 7, which includes the five (or six) individual fitted components and the summed theoretical fit superimposed on the data points. The Mössbauer hyperfine parameters for the fitted components of the five samples are listed in Table 1.

The similarity of the hyperfine parameters for the spectral components of all samples suggests that a similar suite of Fe-phases occurs throughout the reaction, with some exceptions as noted below.

3.4.1. Phases a and b

The magnetic six lines of component a dominate the spectra of all the samples, accounting for nearly 50% of the total spectral area. This component also has the highest internal magnetic field, with the exception of the α - Fe_2O_3 found only at 1500°C. The peaks of this component are significantly broader in the samples fired at 1400 and 1500°C; inspection of the lowest velocity peak shows this broadening to be due to the superposition of at least two different components but it was not feasible to fit this by the addition of a further sextet.

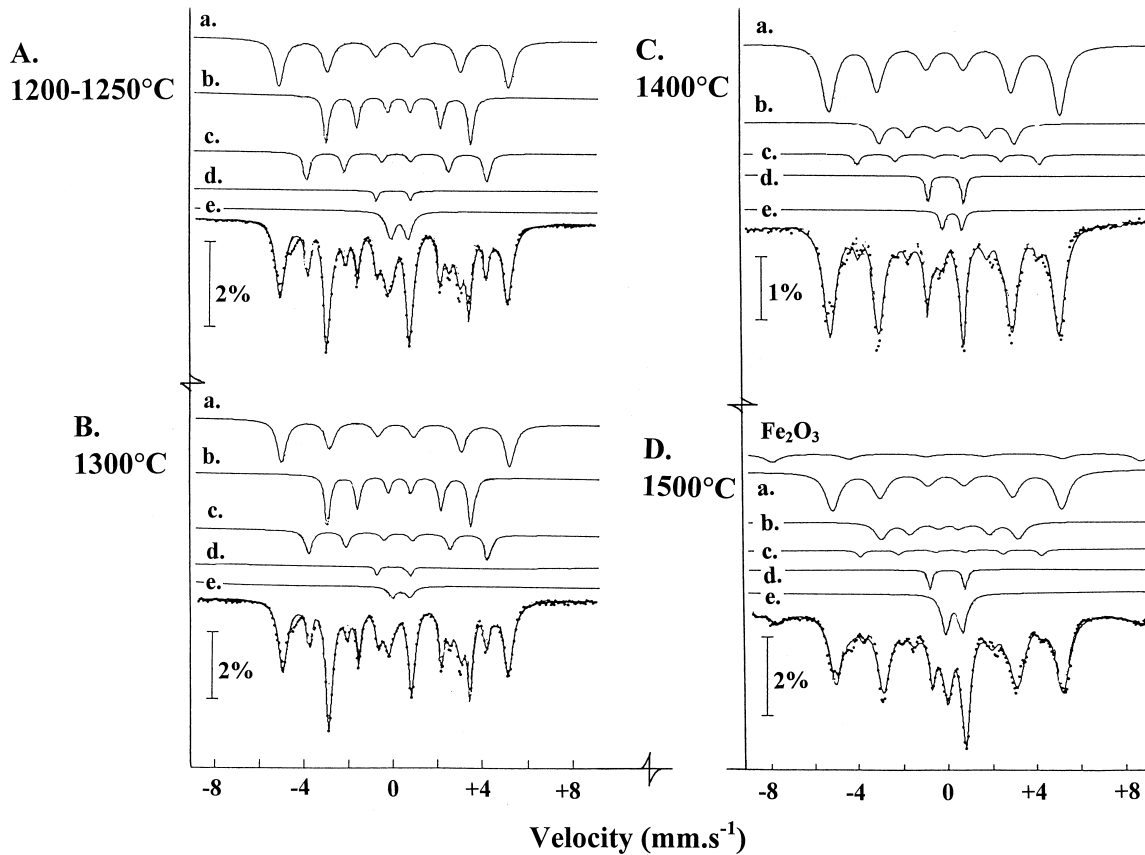


Fig. 7. Typical room-temperature ^{57}Fe Mössbauer spectra of silicothermal X-sialon reaction mixture containing 10 wt.% Fe_2O_3 . Data points with fitted spectral envelope of sub-spectral components shown above. Spectrum A is of the sample fired at 1200°C ; the sample fired at 1250°C is similar.

The relative intensities of the lines of a magnetic sextet in the absence of quadrupole interactions follow the ratio 3:2:1:1:2:3 for a random absorber. The strong intensity of the line near -3.5 mm s^{-1} shows that this line cannot be due solely to component a, and must therefore be due to a second relatively abundant component with quite similar hyperfine parameters. Changes in the intensity of the line at about -1.7 mm s^{-1} are also related to this phase, and suggest that its abundance is dramatically reduced at $1400\text{--}1500^\circ\text{C}$. The Mössbauer hyperfine parameters of phases a and b suggest that these are a mixture of Fe_3Si and Fe_3Al . This identification can be reconciled with the XRD analyses of these samples, which indicate the presence of significant amounts of silicides such as Fe_3Si (Fig. 3D); the presence of Fe_3Al is not however ruled out by XRD, since its powder pattern (PDF no. 45-1203) is quite similar to that of Fe_3Si . The position of the diagnostic XRD silicide peak at about $52.5\text{--}53^\circ 2\theta$ is biased towards the position of Fe_3Si ($53.16^\circ 2\theta$) at 1200°C , but moves towards the position of Fe_3Al ($51.8^\circ 2\theta$) at higher temperatures. Since this XRD reflection is not a perfect match with either of these compounds, the additional occurrence of Fe_3Al became apparent only from the Mössbauer evidence. However, the Mössbauer identification is complicated by

the fact that each of these compounds on its own gives a Mössbauer spectrum consisting of more than one six-line spectral component, of which the number and relative intensity varies with the Al/Si composition. For this reason it is not practicable to further deconvolute the Mössbauer data to gain information about the relative abundance and stoichiometries of these two phases. The simplification adopted here of fitting the spectra of Fe_3Si and Fe_3Al to only two sextets is the probable reason for the few regions of spectral misfit, where the shape of the lines suggests the presence of additional spectral components. However, the addition of more sextets to the fitting model would not alter the conclusion that these two phases dominate the Mössbauer spectra at all temperatures, and would provide no additional information about their relative abundance or stoichiometry.

3.4.2. Phase c

The existence of this component is clearly evident from the peaks at about -4 and $+4 \text{ mm s}^{-1}$; there is no physically realistic combination of parameters that would allow these peaks to belong to components a or b. The well-defined, relatively narrow linewidth is consistent for all the samples and suggests a single phase

Table 1
Mössbauer hyperfine parameters for the Fe-containing phases in fired silicothermal X-sialon mixtures containing 10 wt.% Fe₂O₃

Temperature	Component	Internal field (T)	CS ^a (mm s ⁻¹)	QS (mm s ⁻¹)	FWHH ^b (mm s ⁻¹)
1200°C	a	31.57(1)	0.077(5)	–	0.520(5)
	b	19.85(1)	0.257(5)	–	0.294(5)
	c	24.82(1)	0.195(5)	0.012(5)	0.326(5)
	d	–	0.036(5)	1.51(1)	0.18(1)
	e	–	0.319(5)	0.759(5)	0.44(1)
1250°C	a	31.72(1)	0.078(5)	–	0.078(5)
	b	19.93(1)	0.258(5)	–	0.267(5)
	c	24.87(2)	0.197(5)	0.002(5)	0.30(1)
	d	–	0.02(4)	1.59(7)	0.349(5)
	e	–	0.36(3)	0.87(5)	0.43(3)
1300°C	a	31.51(2)	0.080(5)	–	0.504(6)
	b	19.89(1)	0.257(5)	–	0.294(5)
	c	24.83(2)	0.196(5)	0.006(5)	0.359(7)
	d	–	0.02(1)	1.50(2)	0.18(2)
	e	–	0.32(1)	0.75(2)	0.43(3)
1400°C	a	32.08(2)	0.039(5)	–	0.681(7)
	b	18.71(4)	0.125(6)	–	0.50(2)
	c	25.17(6)	0.197(8)	–	0.33 ^c
	d	–	0.036(5)	1.60(1)	0.20(1)
	e	–	0.339(9)	0.87(2)	0.26(2)
1500°C	a	31.71(2)	0.032(5)	–	0.759(6)
	b	18.98(3)	0.168(5)	–	0.66(1)
	c	24.99(4)	0.204(6)	–	0.33 ^c
	d	–	0.041(5)	1.56(1)	0.227(7)
	e	–	0.334(5)	0.75(1)	0.456(6)
	Fe ₂ O ₃	50.95(6)	0.415(6)	–	0.84(4)

^a Centre shift relative to α -Fe metal.

^b Full width at half maximum height.

^c Held fixed during fitting process.

containing high-spin Fe³⁺, possibly in tetrahedral coordination. The relatively low internal field rules out a simple iron oxide, but the spectrum may arise from another iron silicide or aluminide. The abundance of this component decreases at 1400–1500°C.

3.4.3. Phase d

The presence of this component is inferred from the strong inner peak at about -0.8 mm s⁻¹ of which the other branch of the doublet was sought within the intense feature at ca. $+0.8$ mm s⁻¹. The resulting fit indicates a quadrupole doublet with a rather small centre shift (CS) which could correspond either to Fe⁴⁺ or to very fine superparamagnetic particles of a magnetic alloy such as Fe₃Si or Fe₃Al dispersed in a non-magnetic matrix. The species Fe⁴⁺ is known to occur in Sr₂FeO₄, Ba₂FeO₄ and iron-doped anatase¹⁴ in which it displays a small CS with respect to natural Fe but a quadrupole splitting (QS) value (2.0 – 2.6 mm s⁻¹) somewhat larger than found in the present spectra. On this basis, and from a consideration of its formation chemistry Fe⁴⁺ appears a less likely assignment. Superparamagnetic

Mössbauer spectra have previously been reported¹⁵ in a variety of iron-containing oxide and silicate systems heated under reducing conditions and arise when particles of a magnetic phase are dispersed in an insulating matrix such that their relaxation time becomes smaller than the measurement time of the Mössbauer event (2×10^{-8} s). The present doublet d could arise from fine (< 1000 nm) superparamagnetic particles of a phase with a quadrupole splitting, such as the magnetic phases a or b. The matrix in which these particles are located could be either mullite or sialon. There is Mössbauer evidence for the presence of iron in the substitutional sites of the mullite content of the present samples (see below), but resonance d could represent the iron associated with the X- and O'-sialons known by XRD to be present. This suggestion appears reasonable, although since nothing is currently known about the Mössbauer spectra of iron in sialon, it cannot presently be confirmed. Since the CS value of a magnetic phase is unchanged when it becomes superparamagnetic, the present superparamagnetic particles could be of phase a composition, on the basis of the similarity of its CS to that of doublet d.

3.4.4. Phase e

The Mössbauer parameters of this component are similar to those of the spectrum reported for mullite containing Fe-for-Al substitution¹⁵ in which a broad doublet having similar parameters to component e was fitted to three overlapping doublet corresponding to the single octahedral and two tetrahedral sites of mullite. Although fitting of additional doublets to the present component e was not practicable because of the complexity of the spectra, the identification of this spectral component with the total envelope of mullite resonances seems sound, and the increase in its relative area with temperature is also consistent with the XRD evidence of increased mullite formation at 1500°C (Fig. 2A).

To a first approximation, the areas of the Mössbauer spectral components of a single phase with many sites give an estimate of the relative Fe population of those sites. For a multiple phase system, the situation is complicated by factors such as the variability of Fe abundance in the various phases, sample thickness, recoil-free fraction and sample homogeneity. Nevertheless, the spectral areas of each phase can provide a qualitative indication of the relative abundance of the phase, based on its Fe-content. The relative areas of the spectral components are plotted in Fig. 8 as a function of the firing temperature.

Fig. 8 shows that throughout the reaction the iron-containing phases are predominantly magnetic, especially spectral components a and b, which represent a mixture of Fe₃Si and Fe₃Al. At 1300–1400°C, component a undergoes a significant increase in intensity, with a corresponding decrease in component b. Between 1400 and 1500°C, component a again decreases, accompanied

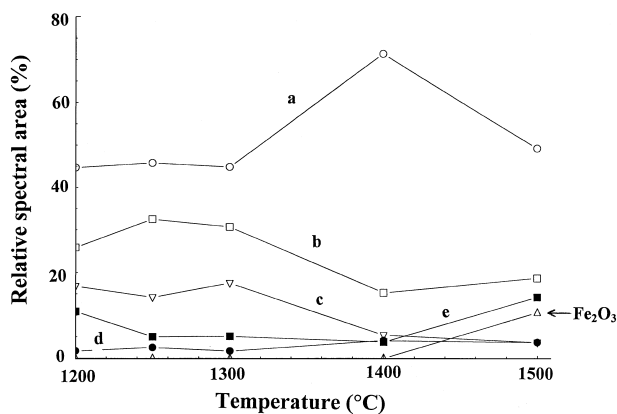


Fig. 8. Relative areas of the fitted Mössbauer sub-spectral components as a function of heating temperature.

by an increase in component e, (iron-substituted mullite) and the appearance of a small amount of free Fe₂O₃. The concentration of minor component d (tentatively identified with superparamagnetic silicide particles possibly in association with X-sialon) remains largely unchanged during the reaction.

4. Conclusions

1. Comparison of the silicothermal formation and sintering of X-sialon in mixtures containing 1 and 10 wt.% MgO, Y₂O₃ and Fe₂O₃ indicate that the trends in the formation of mullite, its subsequent conversion to X-sialon and the sintering behaviour are essentially independent of the additive concentration.

2. The greatest effect on densification is found with 10 wt.% Y₂O₃, followed by MgO and Fe₂O₃; at this oxide concentration the maximum densities are higher than with 1 wt.% oxide, and are achieved at lower temperature (by 1400°C).

3. Both MgO and Y₂O₃ lower the temperatures at which mullite appears and is replaced by X-sialon, by forming liquid phases which facilitate diffusion within the system. Fe₂O₃ enhances the formation and stability of mullite by substitution for Al in the mullite lattice, but suppresses its conversion to X-sialon by preferentially forming Fe silicides at low temperatures, depleting the reacting system of elemental Si.

4. In the presence of 10 wt.% MgO, mullite formation is restricted to that resulting from kaolinite decomposition, since the γ -alumina in the mixture is consumed by reaction with Mg which diffuses into its cubic spinel oxygen lattice, forming MgAl₂O₄. The ²⁵Mg MAS NMR spectra of these samples are consistent with a Mg silicate glass also containing nitrogen. The Mg also promotes the formation of X-sialon containing more SiO₂N₂ units than in the control samples without added MgO.

5. Similarly, the presence of 10 wt.% Y₂O₃ promotes the formation of SiO₂N₂ units in the X-sialon, possibly related to the fact that these are also the structural units of the Y-rich phase *N*-melilite (Y₂Si₃O₃N₄). The ⁸⁹Y and ²⁹Si MAS NMR spectra suggest that the Si-rich liquid occurring in these samples may be of *N*-melilite composition; its formation depletes the system of Si and leads to the transformation of the excess γ -alumina to α -alumina (corundum) above 1300°C.

6. The presence of 10 wt.% Fe₂O₃ leads to the low-temperature formation of a mixture of magnetic phases such as Fe₃Si and Fe₃Al, depleting the system of elemental Si needed for the formation of silicon nitride and hindering the silicothermal transformation to X-sialon of the mullite formed from the clay. The Fe also enters and apparently stabilises the mullite structure by substituting for the lattice Al. There is no unambiguous Mossbauer evidence for the entry of Fe into such X-sialon as is formed in this system, although very fine superparamagnetic particles of silicide which may be responsible for an unusual Mössbauer resonance with a CS value close to zero could be located in the sialon matrix.

References

1. Sheppard, C. M., MacKenzie, K. J. D. and Ryan, M. J., The physical properties of sintered X-phase sialon prepared by silicothermal reaction bonding. *J. Eur. Ceram. Soc.*, 1998, **18**, 185–191.
2. Zhou, Y., Vleugels, J., Lanoui, T., Ratchev, P. and Van der Biest, O., Preparation and properties of X-sialon. *J. Mater. Sci.*, 1995, **30**, 4584–4590.
3. Sheppard, C. M., MacKenzie, K. J. D., Barris, G. C. and Meinhold, R. H., A new silicothermal route to the formation of X-phase sialon: the reaction sequence in the presence and absence of Y₂O₃. *J. Eur. Ceram. Soc.*, 1997, **17**, 667–673.
4. Sheppard, C. M. and MacKenzie, K. J. D., Silicothermal synthesis and densification of X-sialon in the presence of metal oxide additives. *J. Eur. Ceram. Soc.*, 1999, **19**, 535–541.
5. MacKenzie, K. J. D., Meinhold, R. H., White, G. V., Sheppard, C. M. and Sherriff, B. L., Carbothermal formation of β' -sialon from kaolinite and halloysite studied by ²⁹Si and ²⁷Al solid state MAS NMR. *J. Mater. Sci.*, 1994, **29**, 2611–2619.
6. MacKenzie, K. J. D. and Meinhold, R. H., Role of additives in the sintering of silicon nitride: a ²⁹Si, ²⁷Al, ²⁵Mg and ⁸⁹Y MAS NMR and X-ray diffraction study. *J. Mater. Chem.*, 1994, **4**, 1595–1602.
7. MacKenzie, K. J. D. and Meinhold, R. H., Additive-assisted pressureless sintering of carbothermal β' -sialon: an X-ray and solid-state MAS NMR study. *J. Mater. Chem.*, 1996, **6**, 821–831.
8. MacKenzie, K. J. D. and Meinhold, R. H., ²⁵Mg nuclear magnetic resonance spectroscopy of minerals and related inorganics: a survey study. *Am. Mineral.*, 1994, **79**, 250–260.
9. Meinhold, R. H. and MacKenzie, K. J. D., Effect of lanthanides on the relaxation rates of ⁸⁹Y and ²⁹Si in yttrium silicon oxynitride phases. *Solid State Nucl. Magn. Reson.*, 1995, **5**, 151–161.
10. Schneider, H. and Rager, H., Iron incorporation in mullite. *Ceram. Int.*, 1986, **12**, 117–125.
11. Dupree, R. and Smith, M. E., Solid-state magnesium-25 NMR spectroscopy. *J. Chem. Soc., Chem. Commun.*, 1988, 1483–1485.

12. Dupree, R., Lewis, M. H. and Smith, M. E., High-resolution silicon-29 nuclear magnetic resonance in the Y-Si-O-N system. *J. Am. Chem. Soc.*, 1988, **110**, 1083–1087.
13. Dupree, R. and Smith, M. E., Structural influences on high-resolution yttrium-89 NMR spectra of solids. *Chem. Phys. Lett.*, 1988, **148**, 41–44.
14. MacKenzie, K. J. D. and Bowden, M. E., The evolution of an unusual superparamagnetic Mossbauer resonance in iron-containing oxide and silicate systems. *J. Mater. Sci. Lett.*, 1983, **2**, 317–324.
15. Cardile, C. M., Brown, I. W. M., MacKenzie, K. J. D. Mossbauer spectra and lattice parameters of iron-substituted mullites. *J. Mater. Sci. Lett.*, 1987, **6**, 357–362.